



Title	Evolutionary origins of teeth in jawed vertebrates: conflicting data from acanthothoracid dental plates ('Placodermi')
Authors	Meredith Smith, M; Clark, B; Goujet, D; Johanson, Z
Description	© The Authors. Palaeontology published by John Wiley & Sons Ltd on behalf of The Palaeontological Association. doi: 10.1111/pala.12318 829. This is an open access article under the terms of the Creative Commons Attribution License, which permits use, distribution and reproduction in any medium, provided the original work is properly cited.
Date Submitted	2018-03-12



EVOLUTIONARY ORIGINS OF TEETH IN JAWED VERTEBRATES: CONFLICTING DATA FROM ACANTHOTHORACID DENTAL PLATES ('PLACODERMI')

by MOYA MEREDITH SMITH^{1,2}, BRETT CLARK², DANIEL GOUJET³ and ZERINA JOHANSON² 

¹Dental Institute, Tissue Engineering & Biophotonics, King's College London, London, UK; moya.smith@kcl.ac.uk

²Department of Earth Sciences, Natural History Museum, London, UK

³UMR 7207 CR2P CNRS/MNHN/UPMC, Muséum national d'Histoire naturelle, 8 rue Buffon, Paris 05, France

Typescript received 23 November 2016; accepted in revised form 11 June 2017

Abstract: Placoderms (Devonian fossil fishes) are resolved phylogenetically to the base of jawed vertebrates and provide important evidence for evolutionary origins of teeth, particularly with respect to the Arthrodira. The arthrodires represent a derived group of placoderms; the dentition of other more primitive placoderms such as the acanthothoracids is less well known. Articulated acanthothoracid dental plates are rare; x-ray computed tomography of a single, unique specimen, along with 3D segmentation of bone, oral denticles and vascular spaces, provides intrinsic developmental and topological information relevant to tooth origins. Recently, a disarticulated element was identified as a dental

plate of the acanthothoracid *Romundina stellina*, with synchrotron microtomography providing characters to comment on ongoing debates regarding the evolution of teeth. We used segmental quantitative methods to re-analyse this data, for comparison to the articulated and unquestionable acanthothoracid dental plates above. We demonstrate substantial differences between these, disputing the identity of the isolated plate of *R. stellina* as a dental plate, and thus its relevance to questions of tooth evolution.

Key words: Placoderm, dentition, acanthothoracid, *Romundina*, teeth, Devonian.

CURRENT jawed vertebrate phylogenies resolve the fossil group 'Placodermi' as paraphyletic, with the acanthothoracids as one of the more basal groups among the gnathostomes (Giles *et al.* 2015; Qiao *et al.* 2016; but see King *et al.* 2017) and relevant to the evolution of gnathostome characters, for example, teeth and dentitions. However, until recently, the acanthothoracid dentition was known only from a single specimen of the headshield with *in situ* anterior supragnathals (ASGs) articulated to the chondrocranium (Smith & Johanson 2003a; Goujet & Young 2004; Johanson & Smith 2005; Rücklin & Donoghue 2015a). Denticles on these elements presented an organization unlike the tubercles of the dermal armour, representing a distinct, independent oral population, and said to demonstrate a pre-pattern, or blueprint, for gnathostome dentitions as centripetally organized denticles (Smith & Johanson 2003a; Johanson & Smith 2005). These were compared with ordered denticle rows in the gnathal plates of the phylacteniid arthrodire *Dicksonosteus arcticus* (Goujet 1975) with regular

conical denticles increasing in size along the numerous, centripetally (radially) arranged rows (Johanson & Smith 2005). These rows are refined in other arthrodire dentitions showing reduced numbers of rows (Smith & Johanson 2003a, b; Johanson & Smith 2005; Rücklin *et al.* 2012). However, other researchers disagreed, maintaining that morphological similarities existed between oral denticles and dermal shield tubercles, suggesting these had shared origins, both developmental and evolutionary (Goujet & Young 2004; Rücklin & Donoghue 2015a). Thus, interpretation of oral denticles in gnathal plates in acanthothoracids, as basal gnathostomes, is controversial.

Rücklin & Donoghue (2015a) recently compared the published figures of the ASGs of the articulated acanthothoracid (Smith & Johanson 2003a; Goujet & Young 2004) to disarticulated bony plates from a rock residue sample originally associated with the acanthothoracid species *Romundina stellina* (Ørving, 1975), identifying among these a putative upper gnathal plate. This identification was based on similarity in shape to the articulated

acanthothoracid ASGs, and differences with respect to the dermal trunk scales associated with *R. stellina*. This identification was criticized by Burrow *et al.* (2016), in part on the basis of the shape of the convex aboral surface of the *R. stellina* gnathal plate, compared to the strongly concave aboral surface of a Lower Devonian arthrodire gnathal plate (Young *et al.* 2001). In their response, Rücklin & Donoghue (2016) noted that the aboral surface shape in acanthothoracids would not necessarily have been similar to that of the arthrodires, and that the only way to resolve this question would be to examine the acanthothoracid specimen with articulated *in situ* gnathal plates.

Here, these unique acanthothoracid articulated ASGs are analysed with qualitative and quantitative data from new x-ray tomography, and compared with a reanalysis of the original synchrotron data from the putative gnathal plate of Rücklin & Donoghue (2015a). We demonstrate multiple differences between these, especially with respect to relative size, shape, denticle arrangement and volume ranges of denticle populations, as well as aboral plate surfaces. In particular, their relationship and attachment to the perichondral ethmoidal bone, including intrinsic and associated vascular spaces. We conclude that the *R. stellina* specimen is not an oral dental plate (supragnathal) but belongs to part of the dermal skeleton (Burrow *et al.* 2016), and that a flat ASG aboral surface is characteristic of the acanthothoracids, very different to the arthrodire condition (contra Burrow *et al.* 2016). Therefore, Rücklin & Donoghue's (2015a, 2016) interpretation of the disarticulated *R. stellina* plate does not inform on the interrelationship of dermal and oral skeletons and hence their conclusions regarding the evolutionary link between teeth and the dermal ornament (non-independence of these) as based on this plate, can no longer be supported.

Institutional abbreviations. CPW, Museum national d'Histoire naturelle, Paris; NRM-PZ, Naturhistoriska Riksmuseet, Stockholm.

MATERIAL AND METHOD

CPW.9A represents the premedian headshield plate (PrM) and partially preserved bony braincase (eth) of an acanthothoracid placoderm, along with articulated gnathal plates (see Smith *et al.* 2017, supplementary information), while NRM-PZ P.1595 and NRM-PZ P.15952 are disarticulated dermal elements, including the putative dental plate and scales assigned to *Romundina stellina* by Rücklin & Donoghue (2015a, 2016); all of these specimens were collected separately from the Early Devonian (Lochkovian) Prince of Wales Island, Arctic Canada (Ørving 1975; Rücklin & Donoghue 2015a). CPW.9A was scanned using a Nikon metrology HMX ST 225 CT scanner, 1.5 mm copper filter, 200 kV (Imaging and Analysis Centre, Natural History Museum, London). This data has been deposited in Dryad (Smith *et al.* 2017). 3D rendering, presented as selected 'virtual' orthogonal sections (Fig. 1B–E, I) and segmentation and reconstruction of relevant hard or soft tissue features of the gnathal and premedian plates (e.g. the vasculature; Fig. 1D, F–H) used Avizo 9.0 (<https://www.fei.com/software/avizo3d/>) and Drishti 2.6 (<https://sf.anu.edu.au/Vizlab/drishti/>); a medium filter was used on the reconstructed data to assist with segmentation. This reconstructed mCT data were compared with the synchrotron CT data of *Romundina stellina* (Rücklin & Donoghue 2015a, b, MR07A, MR014a).

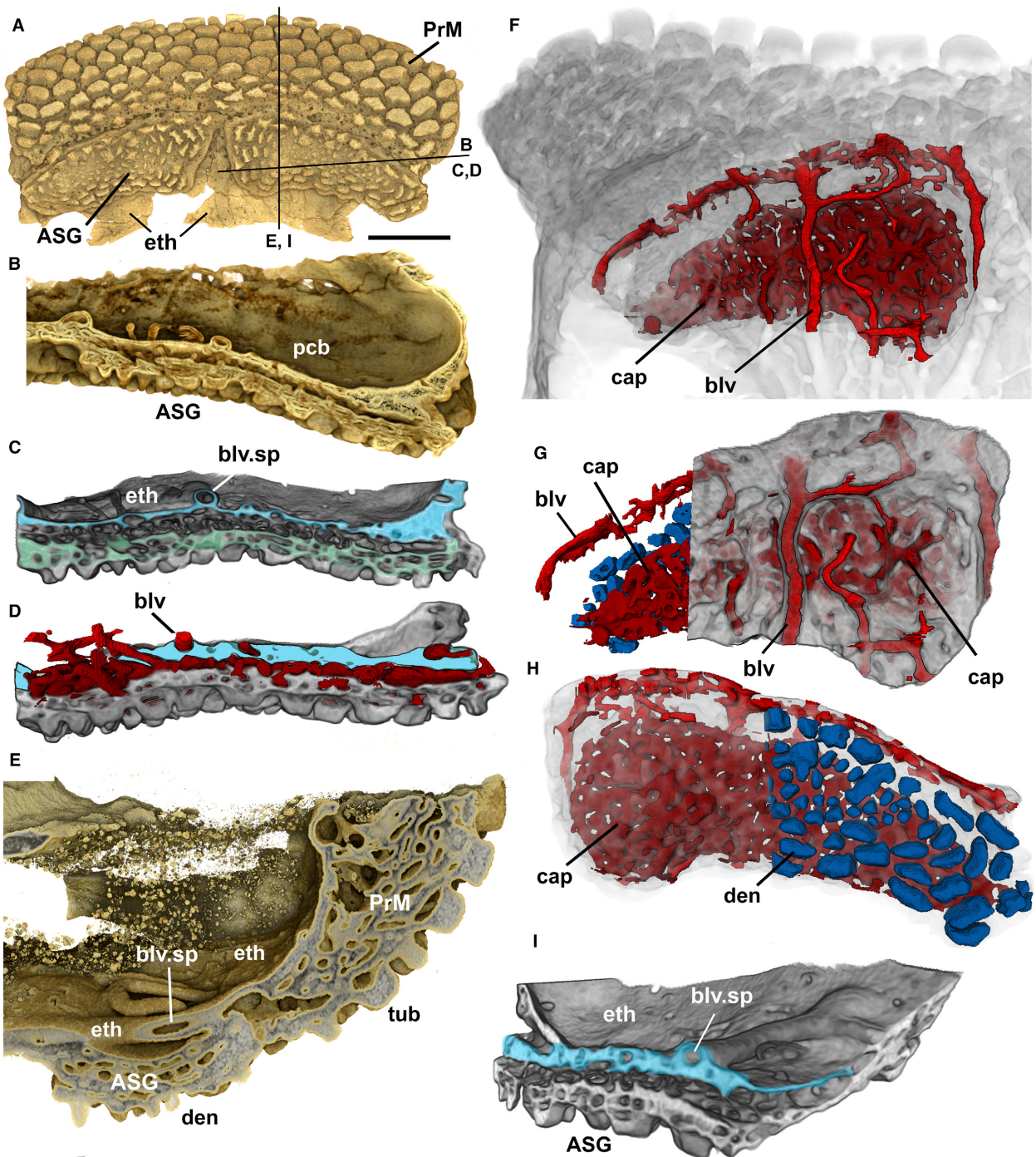
Quantitative analysis

This approach allowed comparisons between tubercles on the ventral PrM margin (nearest the oral cavity) and oral denticles of CPW.9A (left ASG) and the putative oral plate of *Romundina stellina*. All denticles and tubercles were segmented and measured from the point

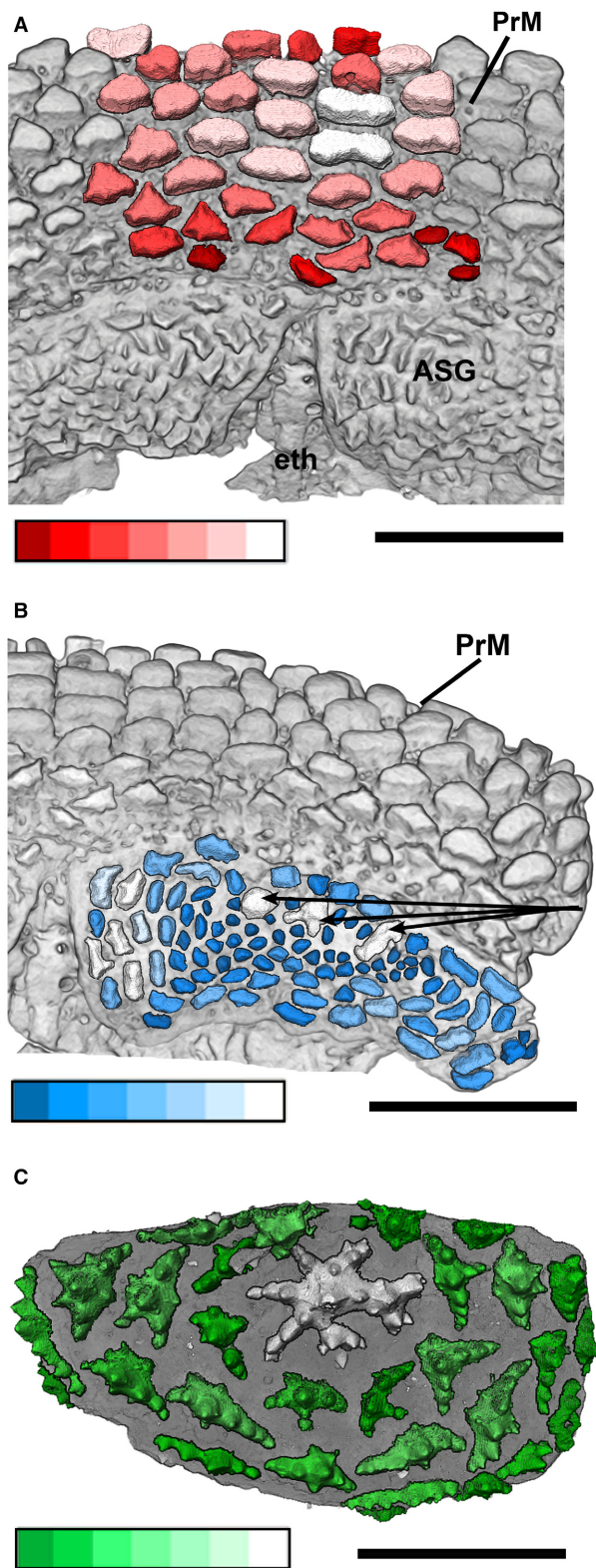
FIG. 1. Acanthothoraci (CPW.9A); 'Placodermi', Prince of Wales Island, Canada (Early Devonian, Lochkovian). A, ventral view of headshield showing premedian plate (PrM) with dermal tubercles, fragments of the ethmoid region of the braincase (eth), and paired, symmetrical, quadrangular anterior supragnathals (ASG) with oral denticles in packed concentric arrays. Lines across PrM and ASG indicate virtual section planes in B–E, I. B, section plane shows tissues of chondrocranial ethmoid and ASG, flat contact surface in this region reflects that of perichondral bone. C–D, orthogonal views of ethmoidal chondrocranium (blue) and gnathal plate on either side of the line through the ASG; C, section with 3D ethmoid demonstrating relationship of ASG to ethmoidal perichondrium via spongy bone (green); D, section of 3D ASG and ethmoid segmented (blue) vascular spaces (red), spongy bone linked to perichondral vessels. E, virtual section through junction of PrM and ASG, showing thickness of spongy bone layer in both; concave junction between ASG and ethmoidal perichondral bone, along with vascular and void spaces within them linking to blood vessel tubes in ethmoidal region (blv.sp). F, aboral view of articulated ASG with bone and tubercles transparent and segmented vascular spaces (red, capillary supply, cap; main blood vessels, blv). G, aboral view of ASG, bone transparent, one-third dissected to show blood supply (blv, cap), denticles blue. H, oral surface denticles (blue) with one-third dissected from oral surface, bone transparent. I, virtual sections along two planes normal to each other; showing segmented ethmoidal perichondral bone (blue), with ASG and space between for blood vessels and capillary plexus (see D, F–H, red). *Abbreviations:* ASG, anterior supragnathal; blv, blood vessel; blv.sp, blood vessels in ethmoidal region; cap, capillaries; den, denticles; eth, ethmoid region of the braincase; pcb, perichondral bone; PrM, premedian plate; tub, tubercles. Scale bar (A) represents 0.25 cm.

where they join the surface of the attachment bone of the oral and dermal plates, then subjected to volumetric measurements (Avizo sieve analysis). A sub-sampled region of the PrM population was selected; incorporating a similar sized study area to that of the ASG. Comparative quantitative analysis examined the variation in volume within, and between, the three populations (Figs 2, 3). Bin sizes (seven in total) were equally

spaced from the smallest to the largest volume within each of the populations (Fig. 2). Each population was measured individually to allow for more volume bins to be assigned (more bins over a smaller range, as for *R. stellina*) to provide quantitated interpretation of observed volume distribution variation in the denticle populations. Along with this, graphs of raw and binned data, along with box plots (Fig. 3) compare the three



different volume ranges, including the extremely small *R. stellina* (range 0.0–0.0014 mm³) with the other two (0.0–0.07 mm³).



RESULTS

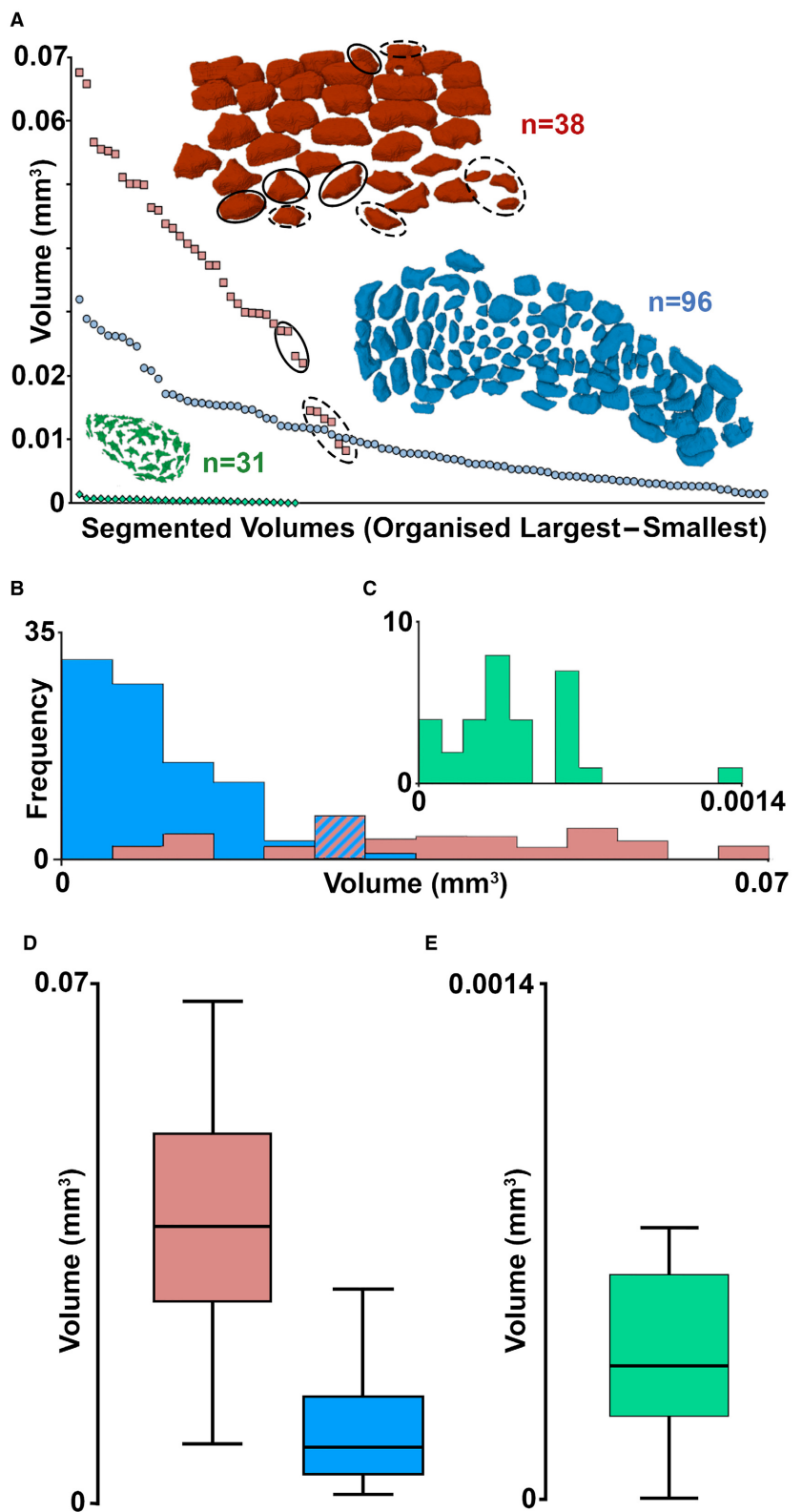
Comparative descriptive morphology

Gnathal denticles on both quadrangular mirror-image ASGs of the acanthothoracid CPW.9A are arranged in a spatially regular manner and centred on the anteromedial focus of the smallest denticle groups. This may reflect growth from the ossification centre, with larger denticles medially and laterally. By comparison, the isolated plate of *Romundina stellina* is ovoid and the largest tubercle is central with radial ridges, arranged as six rows of multiple cusps (Fig. 2C); all other tubercles are smaller and concentric around the largest (with fewer cusps on the radial ridges, Fig. 2C). These concentric tubercles are coincident with the areal growth zones of the bone beneath; each involves addition of tubercle and bone, both apposed to the previous tubercle and bone (Fig. 4F, arrows), whereas no such addition of new denticles with new bone can be visualized in CPW.9A (Fig. 1B). Differences include flat-topped denticles in CPW.9A (none are multicusped) that increase in size centripetally from the central ones (Figs 1A, 2B, 3A) in an apparent radial arrangement from an asymmetric centre. Hence, morphotype, arrangement and growth of denticles, versus tubercles differ in CPW.9A and *R. stellina*.

The aboral attachment surface of the ASGs of CPW.9A (articulating to the mineralized endocranium) is flat to concave depending on the virtual section plane, as the ASG models the endocranial surface (Fig. 1B–E, I; Smith *et al.* 2017, CPW9 movie), very different from the convex basal surface in *R. stellina* (Fig. 4D). The ASGs of CPW.9A are attached through thin trabecular connections of the spongy bone merging with that of the ethmoid region (Fig. 1C, D, blue). Space for large blood vessels in the perichondral bone of the ethmoid region (Fig. 1C, E, blv.sp) indicate that these supply the oral ASG and dermal

FIG. 2. Acanthothoraci, ‘Placodermi’, Prince of Wales Island, Canada (Early Devonian, Lockhovian). Comparative volumes analysed from segmented tubercles and denticles in three distinct colours (mm³; A, red; B, blue; C, green), all with colour gradation from lowest volumes to highest (white). A–B, CPW.9A; C, *Romundina stellina*; NRM-PZ P.15956. A–B, ventral surface of PrM with ASG *in situ*, tubercles red (A), and denticles blue (B), compared with isolated plate tubercles, green (C). Volumes separated into seven size bins: A, PrM plate tubercles, two in white are largest ($n = 38$); B, ASG, all gnathal denticles ($n = 97$), three irregular, larger tubercles interpreted as interpolated onto gnathal plate (black arrows), others white are at medial growth margin. C, isolated plate, tubercles ($n = 31$); largest central tubercle is (white) and none others are this large. *Abbreviations:* ASG, anterior supragnathal; eth, ethmoid region of the brain-case; PrM, premedian plate. Scale bars represent: 0.25 cm (A, B); 178 μ m (E) (Rücklin & Donoghue 2015a).

FIG. 3. Graphs showing distribution of tubercle and denticle volumes (mm^3) of CPW.9A (red, PrM; blue, ASG), and putative suprag-nathal of *Romundina stellina* (green, NRM-PZ P.15956). A, raw data plot showing distribution of volumes, from largest to smallest along the x-axis. PrM tubercles show distinctive size trends, except for the elements within the ellipses (solid line largest, dashed line smallest). B–C, histograms, showing volume distribution and their frequency, of denticles and tubercles in the three populations; B, ASG has a higher frequency of smaller denticles (blue), and PrM (red) a higher frequency of larger tubercles, dashed blue/red overlap zone (as in A, ellipse); C, *R. stellina*, putative suprag-nathal showing a higher frequency of smaller tubercles and separately, one markedly larger tubercle, but all are substantially smaller (A, green) than in CPW.9A. D, box plots showing distribution of tubercle/denticle volumes as in (B–C), indicating that volumes are skewed towards larger values on the PrM, and smaller values on the ASG of CPW.9A, also on the putative suprag-nathal of *R. stellina* (E).



PrM; in general, vascular or void spaces are vast in the spongy bone within both these plates (Fig. 1D, F–H, red), with a network of capillaries (cap) and connective tissue in

the space between the PrM and ASG. In marked contrast, the plate of *R. stellina* possesses a sparse vascular network, dominated by that associated with the large central

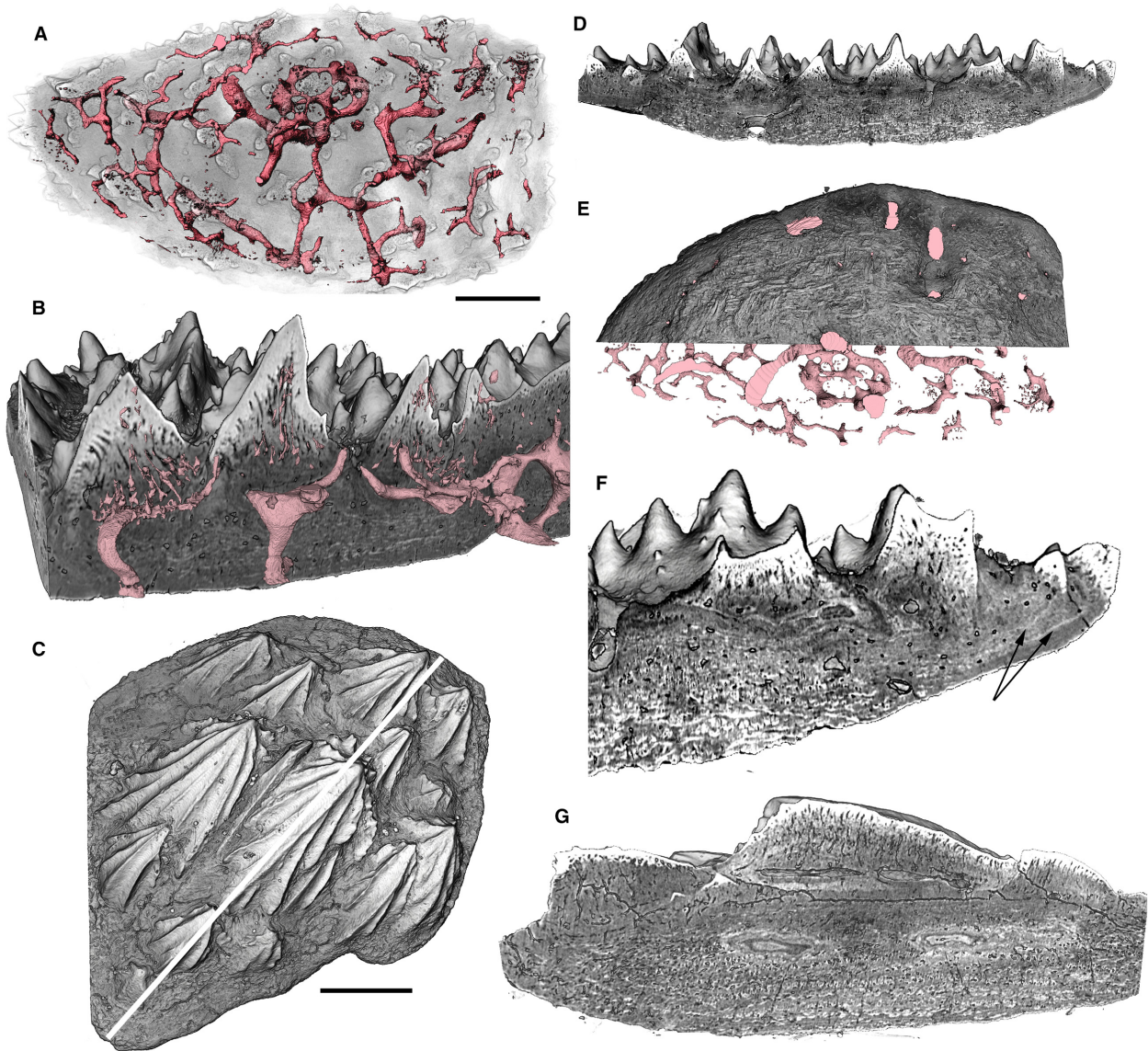


FIG. 4. A, B, D–F, *Romundina stellina* (NRM-PZ P.15956). C, G, NRM-PZ P.15952, 3D volume rendered from synchrotron data (MR07A, MR014a, Rücklin & Donoghue 2015b). A, putative supragnathal showing capillary ring associated with largest tubercle at growth centre and capillaries running to smaller, concentric tubercles (also Rücklin & Donoghue 2016). B, virtual section showing capillaries beneath tubercles, and distribution of capillaries into dentine (pink). C, dermal scale ornamented with ridged tubercles, virtual section plane white line (G). D, virtual section through putative supragnathal, showing convex base (aboral surface). E, aboral surface, showing fibrous tissue composition, capillary network (pink), opening at aboral surface, half shown as network exposed by virtual dissection. F, virtual section through central plane of tubercles with enameloid merging into dentine and arrest lines showing synchronized areal growth associated with tubercle addition (arrows) and support bone. G, central virtual section plane in (C), showing enameloid (with dentine tubules) on each tubercle merging into dentine, and thick lamellar layer basally. Scale bars represent: 240 μm (A, B, D–F); 224 μm (C, G).

tubercle (Fig. 4A, E, pink; Rücklin & Donoghue 2016, fig. 1d) joining a middle vascular network below the tubercles (Fig. 4B, E). The basal bone is a dense, thick compact support tissue (Fig. 4B, D, E; Rücklin & Donoghue 2016, fig. 1a) and differs markedly from the thin spongy bone and flat to concave porous, surface of the ASGs of CPW.9A, which lack a comparable fibrous tissue (Fig. 1B–D, I).

Comparison of denticle populations

Volume calculations of ASG denticles with PrM tubercles of the acanthothoracid CPW.9A, and those on the putative oral plate of *Romundina stellina* compared segmented populations sorted into graded volume bins within each element (Fig. 2). Volumes were also compared between

elements, with raw data plotted, as well as box plots (Fig. 3). With respect to the within-element comparisons, the denticle volumes on the ASG are very small at their growth centre, and larger centripetally towards all margins, with a progressive increase in size from the growth centre outwards (Fig. 2B). This differs from the putative oral plate of *R. stellina*, which shows one large denticle, with the rest being much smaller and all of comparable size (Fig. 2C). On the PrM plate of CPW.9A, tubercle size does not increase in a regular manner centripetally from a growth centre (Fig. 2A). Volume comparisons between the elements show two different populations, with the ASG possessing a larger number of smaller denticles and the PrM with fewer (Figs 2, 3, blue versus red). These populations in CPW.9A differ substantially from the putative oral plate of *R. stellina* (Fig. 3, particularly Fig. 3A).

Nevertheless, the plot of raw volumetric data from CPW.9A shows an overlap of ASG denticle and PrM tubercle volumes, within larger volumes (Fig. 3A, B). This is not unexpected, as denticle size is increasing in a regular manner centripetally as part of the normal ASG development. However, there are regions on the plot of the raw data where the general size trend is irregular (Fig. 3A, ellipses). One of these regions involves the smaller of the PrM tubercles, located near the ASG oral – PrM boundary, the other with the largest of the ASG denticles. The latter includes three denticles near the anterior margin of the ASG (Fig. 2B, arrows). These are similar in volume to dermal tubercles on the PrM but appear interpolated into the regular pattern of oral denticles. Thus, volume overlap may be due to developmental irregularities of both the PrM and ASG that are related to the morphogenetic imprint of dermal, or oral epithelia at this boundary.

DISCUSSION

Rücklin & Donoghue (2015a, 2016) identified a putative dental plate of *Romundina stellina* from acid-prepared rock residues including more typical *R. stellina* dermal plates (Ørvig 1975). Based on morphological differences with respect to dermal trunk armour and scales (e.g. Fig. 4C, F, G) along with a tooth-like composition, they suggested similarities to articulated dental plates in CPW.9A. However, we investigated these dental plates and demonstrated marked morphological differences between the *in situ* articulated dental plates in CPW.9A and the *R. stellina* isolated plate that demonstrate that the latter is not an acanthothoracid dental plate. For example, in CPW.9A, the dental plate has a flatter aboral attachment surface to the perichondral bone of the headshield, compared to the convex basal surface of *R. stellina*. This flat aboral surface may be typical for acanthothoracid

dental plates, and is very different from the strongly concave aboral surface of the early Devonian arthrodiran tooth plate utilized by Burrow *et al.* (2016) in their criticism of the *R. stellina* plate as an oral plate. Importantly, CPW.9A lacks the thick basal lamellar bone present in *R. stellina*, instead possessing a richly vascular spongy bone, linked to major vessels of the ethmoid region. This is very different from the sparse vascular network in *R. stellina*, organized below the central large tubercle and radiating outward to the smaller tubercles, to supply the dentine (Rücklin & Donoghue 2016).

Moreover, our quantitative analysis of ASG oral denticles and PrM dermal tubercles in CPW.9A show differences between the two populations, including notably their organization with a skew towards smaller denticles on the ASG and larger tubercles on the PrM. We suggest that, in principle, larger peripheral denticles on the ASG are the result of the normal, centripetal growth of the plate, with the unusually larger denticles at the rostral border proposed to develop from a disjunct oral–dermal epithelial boundary at this junction.

CONCLUSIONS

We found multiple and distinct differences between the articulated dental plates of the acanthothoracid CPW.9A and the isolated plate of *Romundina stellina* described by Rücklin & Donoghue (2015a, 2016) from 3D segmentation of data obtained from non-invasive x-ray tomography. These differences were determined from quantitative comparisons of odontogenic populations, vascular spaces within the hard tissues, shape of the plate and shape of the aboral surface, along with the tissue composition of the aboral surfaces. We conclude that, compared with the articulated dental plate in CPW.9A, the isolated plate of *R. stellina* is not part of the oral skeleton, therefore, it cannot be relevant to discussions regarding the evolutionary origins of teeth.

Moreover, although there is some overlap among the larger denticles and tubercles, in CPW.9A there are differences between the oral plate denticles (particularly at the presumed plate origin and over much of the plate) and dermal premedian plate tubercles; differences which continue to question the evolutionary relationship between teeth and external body scales. Added to this, differences with respect to other known dermal elements (e.g. the stellate morphology associated with the tubercles) are notable. Testing of evolutionary hypotheses of the interdependence of dermal and oral dentine based tissues will be facilitated by new, precisely described, comparative quantitative differences between dermal and oral denticulated plates in acanthothoracid placoderms.

Acknowledgements. We thank Farah Ahmed and Amin Garbout (Image and Analysis Centre, NHM) for access and assistance with CT-scanning. This work was financially supported by NERC Standard grants NE/K01434X/1754 (ZJ), NE/K014235/1 (MMS). Phil Donoghue and an anonymous referee are thanked for their comments on an earlier version of the manuscript.

Authors' contributions. MMS and BC conceived this study; MMS and ZJ CT-scanned *Romundina*; BC volume rendered CT-data and performed the volumetric calculations; all authors contributed to writing of the manuscript; DG prepared the specimens.

DATA ARCHIVING STATEMENT

Synchrotron scans of *Romundina stellina* are available at <https://doi.org/10.5523/bris.7h9gynbsui4u1hap471inrlua>; mCT-scans of CPW.9A are available in the Dryad Data Repository, along with supporting information and movies: <https://doi.org/10.5061/dryad.hr718>.

Editor. Andrew Smith

REFERENCES

- BURROW, C., HU, Y. and YOUNG, G. C. 2016. Placoderms and the evolutionary origin of teeth: a comment on Rücklin & Donoghue (2015). *Biology Letters*, **12**, 20160159.
- GILES, S., FRIEDMAN, M. and BRAZEAU, M. D. 2015. Osteichthyan-like cranial conditions in an Early Devonian stem gnathostome. *Nature*, **520**, 82–85.
- GOUJET, D. 1975. *Dicksonosteus*, un nouvel arthrodire du Dévonien du Spitsberg: remarques sur le squelette visceral des Dolichothoraci. *Colloques Internationaux du Centre National de la Recherche Scientifique*, **218**, 81–99.
- and YOUNG, G. C. 2004. Placoderm anatomy and phylogeny: new insights. 109–126 In ARRATIA, G., WILSON, M. V. H. and CLOUTIER, R. (eds). *Recent advances in the origin and early radiation of vertebrates*. Verlag Dr Friedrich Pfeil.
- JOHANSON, Z. and SMITH, M. M. 2005. Origin and evolution of gnathostome dentitions: a question of teeth and pharyngeal denticles in placoderms. *Biological Reviews*, **80**, 303–345.
- KING, B., QIAO, T., LEE, M. S. Y., ZHU, M. and LONG, J. A. 2017. Bayesian morphological clock methods resurrect placoderm monophyly and reveal rapid early evolution in jawed vertebrates. *Systematic Biology*, **66**, 499–516.
- ØRVIG, T. 1975. Description, with special reference to the dermal skeleton, of a new radotinid arthrodire from the Gedinnian of Arctic Canada. *Colloque International CNRS*, **218**, 41–71.
- QIAO, T., KING, B., LONG, J. A., AHLBERG, P. E. and ZHU, M. 2016. Early gnathostome phylogeny revisited: multiple method consensus. *PLoS One*, **11**, e0163157.
- RÜCKLIN, M. and DONOGHUE, P. C. J. 2015a. *Romundina* and the evolutionary origin of teeth. *Biology Letters*, **11**, 20150326.
- and DONOGHUE, P. 2015b. Dataset: *Romundina* and the evolutionary origin of teeth. University of Bristol. <https://doi.org/10.5523/bris.7h9gynbsui4u1hap471inrlua>
- — 2016. Reply to ‘placoderms and the evolutionary origin of teeth’: Burrow *et al.* (2016). *Biology Letters*, **12**, 20160526.
- DONOGHUE, P. C. J., JOHANSON, Z., TRINAJSTIC, K., MARONE, F. and STAMPANONI, M. 2012. Development of teeth and jaws in the earliest jawed vertebrates. *Nature*, **491**, 748–751.
- SMITH, M. M. and JOHANSON, Z. 2003a. Response to comment on “Separate evolutionary origins of teeth from evidence in fossil jawed vertebrates”. *Science*, **300**, 1661.
- — 2003b. Separate evolutionary origins of teeth from evidence in fossil jawed vertebrates. *Science*, **299**, 1235–1236.
- CLARK, B., GOUJET, D. and JOHANSON, Z. 2017. Data from: Evolutionary origins of teeth in jawed vertebrates: conflicting data from dental plates in the placoderm *Romundina*. *Dryad Digital Repository*. <https://doi.org/10.5061/dryad.d357k>
- YOUNG, G. C., LELIÈVRE, H. and GOUJET, D. 2001. Primitive jaw structure in an articulated brachythoracid arthrodire (placoderm fish; Early Devonian) from southeastern Australia. *Journal of Vertebrate Paleontology*, **21**, 670–678.